frontiers in Earth Science

REVIEW
published: 18 March 2022
doi: 10.3389/feart.2022.837775

Fate of Carbonates in the Earth's Mantle (10-136 GPa)

Jing Gao[1]*, *Xiang Wu*[2], *Xueyin Yuan*[3] and *Wen Su*[1]

[1]State Key Laboratory of Lithospheric Evolution, Institutions of Earth Science, Institute of Geology and Geophysics, Chinese Academy of Sciences, Beijing, China, [2]State Key Laboratory of Geological Processes and Mineral Resources, China University of Geosciences, Wuhan, China, [3]MNR Key Laboratory of Metallogeny and Mineral Assessment, Institute of Mineral Resources, Chinese Academy of Geological Sciences, Beijing, China

Earth carbon cycle shapes the evolution of our planet and our habitats. As a key region of carbon cycle, subduction zone acts as a sole channel transporting supracrustal carbonate rocks down to the mantle, balancing carbon budget between the Earth's surface and the interior, and regulating CO_2 concentration of the atmosphere. How carbonates evolve at depth is thus, a most fundamental issue in understanding carbon flux and carbon sequestration mechanism in the Earth. This study reviews prominent progresses made in the field of crystal chemistry of carbonates along subduction geotherms. It clearly finds that, in addition to common carbonates in the Earth's crust, several new polymorphs of carbonates have been discovered to be stable under high-pressure and high-temperature conditions. This opens possibilities for oxidized carbon species in the deep Earth. However, metamorphic decarbonatation and reduction reactions restrict subducting carbonates to the top-mid region of the lower mantle. Specifically, subsolidus decarbonatation in the form of carbonates reacting with silicates has been proposed as an efficient process releasing CO_2 from slabs to the mantle. Besides, carbonate reduction in the metal-saturated mantle likely results in generation of super-deep diamonds and a considerable degree of carbon isotope fractionation. Review of these novel findings leads us to consider three issues in the further studies, including *1*) searching for new chemical forms of carbon in the mantle, *2*) determining the reduction efficiency of carbonates to diamonds and the accompanying carbon isotope fractionation and *3*) concerning carbon cycle in subduction of continental crust.

Keywords: phase relation, crystal chemistry, diamond, graphite, decarbonatation

OPEN ACCESS

Edited by:
Guibin Zhang,
Peking University, China

Reviewed by:
Renbiao Tao,
Center for High Pressure Science and Technology Advanced Research, China
Yi-Xiang Chen,
University of Science and Technology of China, China
Michel Grégoire,
UMR5563 Géosciences Environnement Toulouse (GET), France

***Correspondence:**
Jing Gao
gaojing@mail.iggcas.ac.cn

Specialty section:
This article was submitted to Petrology, a section of the journal Frontiers in Earth Science

Received: *17 December 2021*
Accepted: *18 January 2022*
Published: *18 March 2022*

Citation:
Gao J, Wu X, Yuan X and Su W (2022) Fate of Carbonates in the Earth's Mantle (10-136 GPa). Front. Earth Sci. 10:837775. doi: 10.3389/feart.2022.837775

INTRODUCTION

Carbon is a basic element that forms the Earth and the biosphere. Earth carbon cycle ties closely with the global climate, the origin and evolution of life and the carbon-based energy resources. The present review focuses on the carbon cycle in subduction zones. The crustal carbon is carried down to the Earth's interior *via* subduction processes, modifying the redox state of the mantle, and the deep carbon exchanges with the crustal carbon *via* volcanism or metamorphic decarburization over geological timescales (Dasgupta and Hirschmann, 2010; Plank and Langmuir, 1993). This process is responsible for the recycling of a great amount of carbon and consequently, exerts profound influence upon the terrestrial ecosystem functions. In recent decades, the carbon balance between the Earth's surface and the interior is wrecked. It has become our urgent desire to examine carbon sequestration capacity of different reservoirs and strive for a balance of carbon income and outcome.

Extensive studies have been carried out on carbon flux from the Earth's surface to the interior but obtained totally different results (Gorman et al., 2006; Johnston et al., 2011). Estimation on the removal amount of the subducted carbon from slabs varies from 35 to 100% (Kelemen and Manning, 2015). The large inconsistency is due mainly to our limited knowledge on behaviors of carbonates in subduction zones.

Carbonates (e.g. calcite $CaCO_3$, magnesite $MgCO_3$ and dolomite (Ca, Mg)CO_3) are predominantly carbon species in the Earth's crust. Their structural stability in subduction zones is a key to measuring carbon flux. On the one hand, with the increase of the subduction depth, the pressure-temperature and the oxygen fugacity conditions become more and more favorable for reduced carbon species. In this respect, carbonates would be overtaken by diamond or graphite at mantle depths in excess of ~250 km where the redox state begins to be buffered by iron-wüstite equilibrium due to disproportionation of Fe^{2+} to Fe^{3+} and metallic Fe^0 (Frost et al., 2004). At greater depths, Fe^{2+} disproportionation to Fe^{3+} and Fe^0 progressively increases, which likely results to diamond domains in the deep Earth (Rohrbach and Schmidt, 2011). On the other hand, however, the possibilities of crustal carbonates in the upper-mid mantle have been suggested by thermodynamic calculations (Sun et al., 2018) and experiments (Ghosh et al., 2009; Litvin et al., 2014). Besides, carbonate associations have been frequently discovered as inclusions in the transition-zone and the lower-mantle diamonds (e.g. Brenker et al., 2007; Kaminsky, 2012; Kaminsky et al., 2013; 2016). This indicates that the crystal chemistry of carbonates and the carbon sequestration mechanism in the deep Earth are far more complicated than previously thought.

In this study, we systematically review the high-pressure behaviors of carbonates along from cold to the hottest subduction geotherms, aiming at three scientific issues: *1*) Establishing a comprehensive phase relation of main carbonates in the Earth's mantle. Our first concern is whether carbonates will melt and breakdown at high-pressure and high-temperature conditions, or preserve to greater depths even approaching the core-mantle boundary (CMB). *2*) Next, close attention are paid upon the reduction mechanism of carbonates in reactions with the metallic mantle during subducting processes, as that would be an impenetrable barrier to carbonate subduction. *3*) Meanwhile, decarbonization of carbonated peridotites and eclogites (including mid-ocean ridge basalt, MORB) by the surrounding silicates should also be examined, as these processes exhibit the possibility of CO_2 release as an equilibrium phase in the deep mantle, which sets fundamental control on mantle metasomatism.

PHASE DIAGRAM OF CARBONATES IN THE MANTLE

$CaCO_3$, $MgCO_3$, (Ca,Mg)CO_3 are three main inorganic carbon substances in the Earth's crust. They are also dominant carbon species recovered in sublithospheric diamonds. Carbonates show versatile behaviors such as phase transition, dissolution, melting, decomposition and decarburization at mantle conditions. For example, $CaCO_3$ exhibits exceeding solubility in aqueous fluids and may extract a considerable portion of carbon from slabs. But Ca^{2+} in carbonates would be replaced by Mg^{2+} upon sinking, and the solubility of dolomite reduces significantly if carbonates become Mg-rich (Farsang et al., 2021). Naturally Fe^{2+} substituting Mg^{2+} forms a complete $MgCO_3$-$FeCO_3$ solid solution, and a minor addition of Fe^{2+} significantly affect the phase boundary of carbonates especially at lower-mantle pressures (Liu et al., 2015; Tao et al., 2014). The following section presents a summary of phase relation of $CaCO_3$, $MgCO_3$ and (Ca,Mg)CO_3 and their ferrous series at depths.

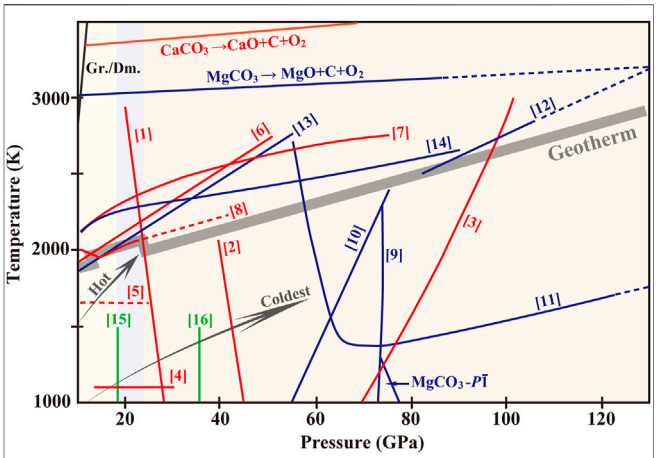

FIGURE 1 | Phase diagram of $CaCO_3$, $MgCO_3$, (Ca,Mg)CO_3 and the ferrous series under high pressures and temperatures. Equilibrium boundary between Gr. and Dm. is based on Bundy et al. (1996). Pressure-Temperature-profiles of hot subduction slab (red arrow) stagnant in the transition zone and the coldest slab (navy-blue arrow) penetrating into the lower mantle (an extrapolated curve) are referred to Syracuse et al. (2010). The gray zone indicates the Mantle Geotherm (Katsura et al., 2010). Curve [1] represents the phase boundary between Arag. and $CaCO_3$-VII and Curve [2] between $CaCO_3$-VII and Post-Arag. (Gavryushkin et al., 2017; Li et al., 2018). Transformation from Post-Arag. to $P2_1/c$-*h* is indicated by Curve [3] (Gavryushkin et al., 2017; Zhang ZG. et al., 2018). Phase relation between $CaCO_3$-VI (*P*-1) and Arag. (13.5–25 GPa; ~1100 K) is denoted by Curve [4] (Pickard and Needs, 2015; Bayarjargal et al., 2018). Curve [5] is an extrapolated curve showing the transformation from Arag. to $CaCO_3$-V (disordered) (Litasov et al., 2017; Zhao et al., 2019) or an unknown structure. Melting curves of $CaCO_3$ and the boundary of decomposition of $CaCO_3$ melt are referred to Litvin et al. (2014) (Curve [6]), Zhang and Liu, (2015) (Curve [7]) and Li et al. (2017) (Curve [8]). Structural evolution from $MgCO_3$ to *C2/m* (Curve [9]) is based on Oganov et al. (2008) and Boulard et al. (2011). $MgCO_3$-*P*-1 has a limited stable regime between 85 and 101 GPa below ~1100 K (Pickard and Needs, 2015). Spin crossover of Fe^{2+} in ferromagnesite (Curve [10]) is from Liu et al. (2015). Phase boundaries from Fe^{2+}-rich Mg-carbonates-*R*-3*c* to *Pmm*2 (Curve [11]) is plotted by Liu et al. (2015) and to *C2/m* (Curve [12]) by Boulard et al. (2011; 2012; 2015). $MgCO_3$ melt and the decomposition to diamond are measured from Litvin et al. (2014) (Curve [13]) and Solopova et al. (2015) (Curve [14]). Phase transition from Fe-Dol. to Fe-Dol.-II is denoted by Curve [15] and further to Fe-Dol.-III by Curve [16] (Merlini et al., 2012). Abbreviations: Gr., graphite; Dm., diamond; Arag., aragonite; Post-Arag., post-aragonite; Fe-Dol., Fe^{2+}-bearing dolomite; Fe-Dol.-II, Fe^{2+}-bearing dolomite-II; Fe-Dol.-III, Fe^{2+}-bearing dolomite-III.

Calcite $CaCO_3$

The stable polymorph of $CaCO_3$ at ambient conditions is calcite (*R*-3*c*, *Z* = 6) where $[CO_3]^{2-}$ species form parallel layers and Ca^{2+} are six-fold coordinated by O^{2-}. Upon pressures above ~2 GPa, calcite reconstructively converts to aragonite (*Pmcn*, *Z* = 4) with $[CaO_6]$-octahedra turning into $[CaO_9]$-polyhedra. Aragonite has long been considered as the dominant $CaCO_3$-structure in the Earth's interior from the upper mantle to the top of the lower mantle. Yet its density is lower than the principle constituents of the mantle (Litasov et al., 2007), which casts doubts on the presence of $CaCO_3$ in the deep Earth. Accumulations of experimental and theoretical data lately, however, create a whole new landscape of $CaCO_3$ inside the Earth. One significant finding is $CaCO_3$-VII ($P2_1/c$-*l*, *Z* = 4), which was put forward by Gavryushkin et al. (2017) as favorable in the pressure range of 30–50 GPa below1200 K (**Figure 1**). Bayarjargal et al. (2018) and Li et al. (2018) subsequently expanded its temperature scope to the melting point and suggest $CaCO_3$-VII as a predominant candidate at mantle depths of 690–1010 km. Increasing temperature would lower the pressure of aragonite → $CaCO_3$-VII transformation (Zhang ZG. et al., 2018). $CaCO_3$-VII is characterized with non-planar $[CO_3]^{2-}$ units that are rotated by ~45° relative to those in calcite/aragonite and are tilted ~90° to one another. It is considered as an intermediate in the aragonite → post-aragonite transformation wherein the $[CO_3]^{2-}$ units undergo a ~90° rotation (Pickard and Needs, 2015; Smith et al., 2018). Conversion of aragonite to $CaCO_3$-VII is accompanied by an uprush of 2% for density, and an increase of 9, 2 and 8% for shear, longitudinal and average sound velocities. The difference in wave velocities increase by ~6% when 10% $CaCO_3$ is present with respect to a pure pyrolitic composition (Bayarjargal et al., 2018). Therefore, the potential preferred orientation of $CaCO_3$-VII may contribute to seismic discontinuities at ~700 km in the vicinity of slabs (Kaneshima, 2013; Yang and He, 2015; Bayarjargal et al., 2018).

In the meanwhile, Gavryushkin et al. (2017) took the initiative in observing the occurrence of aragonite-II ($P2_1/c$), another model structurally relevant to aragonite at 35 GPa and its absence at 50 GPa. The phase domain of aragonite-II was reproduced by Bayarjargal et al. (2018) under non-hydrostatic pressures of 30–38 GPa. Yet never aragonite-II was a pure phase in both studies. By contrast, at pressures of 23–38 GPa, Li et al. (2018) observed only $CaCO_3$-VII generation at temperatures up to 2300 K. Zhang ZG. et al. (2018) provided thermodynamic arguments for the marginal metastability of aragonite-II at 30–40 GPa, and with temperature rising, aragonite-II became increasingly unfavorable. It is open to question for the presence and stability of aragonite-II, which is subjected to kinetic barriers of equilibrium phase transformations in experiments and uncertainties in calculations.

At 42 GPa and 1400 K, a further phase transition occurs from $CaCO_3$-VII to post-aragonite (*Pmmn*, *Z* = 2) with the Clapeyron slope of the phase boundary being -233 K/GPa (Bayarjargal et al., 2018; Li et al., 2018). Post-aragonite exhibits much higher wave velocity anisotropies than major silicates and other carbonates (Huang et al., 2017). This reconstructive transformation leads to measurable decreases in shear (−7.0%) and longitudinal (−4.7%) wave velocities around 1010 km in consideration of the pyrolitic mantle composition with 10% $CaCO_3$ (Li and Yuen, 2014; Niu, 2014; Bayarjargal et al., 2018). Post-aragonite was once believed as the best host structure for $CaCO_3$ in the bulk of the lower mantle and it transformed to a pyroxene-like structure $C222_1$ at the CMB (Oganov et al., 2008). This notion, however, should be deliberated. Another pyroxene-phase $P2_1/c$-*h* as recommended above ~65 GPa, which was evolved from collapse of $P2_1/c$-*l* without energy barriers (Pickard and Needs, 2015; Huang et al., 2017; Zhang ZG. et al., 2018). Both $P2_1/c$-*h* and $C222_1$ are featured with $[CO_4]^{4-}$ species, but the former is made up of pyroxene chains stacked out-of-phase while the latter of parallel chains. In spite of pyroxene-phases, Lobanov et al. (2017) insisted that post-aragonite perseveres until ~105 GPa, afterwards it undergoes the lowest-enthalpy path to become $P2_1/c$-*h* along with conversion of sp^2-to sp^3-hybridized carbon. But Smith et al. (2018) documented that $CaCO_3$-VII itself is capable of sp^2-sp^3 hybridization exchange and rather than any known $CaCO_3$-polymorphs, an entirely new phase came in above ~50 GPa. There exist remarkable discrepancies as to the stability of $CaCO_3$-polymorphs under mid-mantle pressures as well as the phase boundaries, due likely to the kinetic hindrance of the transformations or limitations of different approaches, but sp^3-hybridized carbon does merit special notice because of its thermodynamical stability in the megabar regime.

Melting of $CaCO_3$ was observed at ~1880 K at 3 GPa (Irving and Wyllie, 1975) and monitored using Raman Spectroscopy above ~1900 K at 10 GPa (Litvin et al., 2014), with a smoother slope by conductivity measurement (Li et al., 2017). The melting curve derived from First-principles calculations shifted slightly to lower temperatures, where a knee point occurred at 13 (1) GPa and 1970 (40) K that was attributed to conversion between $CaCO_3$-V and aragonite. Aragonite was detected in the recovered products in the pressure-temperature region where $CaCO_3$-V is supposed to be stable (Zhang and Liu, 2015; Li et al., 2017) due likely to the unquenchable character of $CaCO_3$-V. $CaCO_3$ had a broad area of congruent melting up to ~3500 K, above which, it started to decompose. Decomposition of $CaCO_3$ resulted in generation of graphite that transformed to diamond if annealed to lower temperatures of 700–2700 K (Bayarjargal et al., 2010; Spivak et al., 2011). All these studies pointed out that melting and decomposition of $CaCO_3$ were realized at temperatures above most subduction geotherms. That is, almost the whole mantle falls into the solid regime of $CaCO_3$ polymorphs.

$CaCO_3$ with complex structural chemistry can be understood from the following two perspectives. *1*) In calcite-members ($CaCO_3$, $CdCO_3$, $MnCO_3$, $FeCO_3$, $ZnCO_3$, $MgCO_3$, etc), $CaCO_3$ has the largest ionic radius of Ca^{2+} that can bear various pressures by adjusting coordination numbers (Oganov et al., 2008). *2*) In aragonite-family ($CaCO_3$, $SrCO_3$, $PbCO_3$, $BaCO_3$, etc), $CaCO_3$ contains the closest matching in distance between Ca^{2+} and $[CO_3]^{2-}$ species that results to the most variation in C-O bond lengths and deviation from $[CO_3]^{2-}$-coplane (Antao and Hassan, 2009). The great variety of $CaCO_3$ polymorphs opens possibilities of stable $CaCO_3$ component in the deep mantle. According to the results

above, we plot **Figure 1** for to obtain an overview of phase evolution of $CaCO_3$ to be aragonite (≤~25 GPa) → $CaCO_3$-VII (25–42 GPa) → post-aragonite (42–80 GPa) → $P2_1/c$-h or $C222_1$ (80–137 GPa), which is dominantly affected by pressure.

Magnesite $MgCO_3$ and Ferromagnesite

$MgCO_3$ maintained its rhombohedral structure (R-3c; Z = 6) up to at least ~80 GPa and ~2300 K, thereafter it turned into $MgCO_3$-II ($C2/m$; Z = 6) until the CMB (Isshiki et al., 2004; Maede et al., 2017) (**Figure 1**). $MgCO_3$-II is featured with $[C_3O_9]^{6-}$-rings that consists of three $[CO_4]^{4-}$-tetrahedra with asymmetric C-O bonds, and Mg^{2+} are in eight- or ten-fold coordination (Oganov et al., 2008; Boulard et al., 2011). Another silicate-like polymorph $C222_1$ was once proposed as the most thermodynamically favorable for $MgCO_3$ above ~102 GPa (Panero and Kabbes, 2008), but it was dismissed later. By calculations, Pickard and Needs (2015) suggested a new phase of P-1 to be the best candidate at pressures of 85–101 GPa in a limited temperature regime that is slightly lower than the coldest subduction geotherm. That is the reason why in most attempts we observed $MgCO_3$ directly transformed to $MgCO_3$-II (Boulard et al., 2011; Maeda et al., 2017; Martirosyan et al., 2018). The stability of $C2/m$ was also confirmed in Fe^{2+}-rich $MgCO_3$ (Ferromagnesite-II) above 80 GPa between 1850 and 2500 K. Ferromagnesite-II hasd a higher density and was temperature quenchable. Especially it could accommodate a considerable amount of Fe^{3+} (magnetite Fe_4O_3 and/or a new phase of $Fe_4(CO_4)_3$) that resulted from self-redox reaction between Fe^{2+} and $[CO_3]^{2-}$ (Boulard et al., 2011, 2012, 2015; Chen et al., 2018). Special attention has been paid on spin transition of Fe^{2+} that drives a prior-transformation of ferromagnesite from R-3c to $Pmm2$ at ~50 GPa and 1400 K (Liu et al., 2015), along with an abrupt volume collapse. The phase boundary of ferromagnesite from high spin to low spin state was tightly constrained around 60 GPa for temperatures above ~1000 K (Liu et al., 2015). There might be a positive correlation between the Fe^{2+}-content and the spin transition pressure (Spivak et al., 2014). Or there is just a negligible compositional effect due to the long Fe^{2+}-Fe^{2+} distances in the structure separated by $[CO_3]^{2-}$ species (Lin et al., 2012; Hsu and Huang, 2016; Weis et al., 2017). Some doubts remain regarding the presence of intermediate-spin state (Hsu and Huang, 2016; Weis et al., 2017).

$MgCO_3$ melt congruently at temperatures above the Mantle Geotherm (Litvin et al., 2014; Solopova et al., 2015). An increasing separation in melting points between $CaCO_3$ and $MgCO_3$ with pressure was expected to partially account for the majority of carboantitic melt found on the Earth's surface being highly calcic (Hammouda et al., 2015; Li et al., 2017). $MgCO_3$ decomposed to oxides and diamond above ~3000 K (Spivak et al., 2013; Litvin et al., 2014; Solopova et al., 2015), and the energy cost for $CaCO_3$ is much higher (Santos et al., 2019). Melting curve of ferromagnesite deviated seriously from that of pure $MgCO_3$. Similar to $FeCO_3$, melting loop of ferromagnesite was asymmetrical and had a thermal minimum for Fe^{2+}-rich compositions (Tao et al., 2014; Kang et al., 2015). At mantle conditions, ferromagnesite was energetically advantageous over decomposition (Boulard et al., 2011; 2012), which generated magnetite-magnesioferrite solid solution, graphite and CO_2 (Kang et al., 2016). So melting and decomposition of $CaCO_3$-$MgCO_3$ series bounded the phase fields of these carbonates, and that cast doubts on releasing free CO_2 in the deep Earth.

The elastic behaviors of $MgCO_3$ associate closely to its structural chemistry, which besides, helps to locate the presence of subducted carbonates in the mantle. At mantle pressures, the shear wave velocities in $MgCO_3$ were smaller than those in silicates. Marcondes et al. (2016) thus associated the low-velocity zones near the bottom of the lower mantle with the presence of $MgCO_3$. In the light of the density reduction, Litasov et al. (2008) announced that $MgCO_3$ had a limited effect on seismic profiles of principle assemblages in the mantle, but Yang et al. (2014)proposed to detect its presence by regionally seismic anisotropies because of its unusual high compressional (V_P) and shear (V_S) anisotropies. Existence of minor Fe^{2+} as well as the spin transition opened a new window on the elastic properties of ferromagnesite (Fu et al., 2017; Stekiel et al., 2017). For high spin state, the sound velocities decreased with Fe^{2+}-content, whereas the anisotropy of the sound velocities increased. Upon pressure, anisotropies of V_P and V_S increased until spin transition occurred and decreased afterwards. So a drastic softening of sound velocities across spin transition may occur in slabs enriched with ferromagnesite in the mid-lower mantle. Increases of both V_P and V_S velocities were observed after spin transition. Enrichment of Fe^{2+} led to larger differences in sound velocities and velocity anisotropies for low spin state as well. In this regard, Fe^{2+}-rich $MgCO_3$ regions may show higher seismic contrast compared with principle minerals in the deep mantle.

To sum up (**Figure 1**), along subduction geotherms $MgCO_3$ maintains initial R-3c structure up to ~80 GPa and hereafter converts to $C2/m$, with sp^2-sp^3 transition further upholding the phase in the lowermost mantle. Ferromagnesite undergoes spin transition in the mid-mantle and changes to $Pmm2$-structure subsequently. The drop in the unit-cell and the accordingly uprush of the density expand the stability field of ferromagnesite to higher pressures, yet disproportionation of Fe^{2+} could highly disintegrate the structure at lower-mantle conditions. Temperature exerts a greater impact on phase relations of ferromagnesite relative to $MgCO_3$. Neither melting nor decomposition occurs in $MgCO_3$ or ferromagnesite over the entire mantle.

Dolomite $(Ca,Mg)CO_3$ and Ankerite

Dolomite-$(Ca,Mg)CO_3$ is a common carbonate mineral in marine sediments, carbonated eclogite and ophiolite (Tao et al., 2020; Shatskiy et al., 2021). At the topmost of the upper mantle, dolomite broke down into a mixture of magnesite-$MgCO_3$ and aragonite-$CaCO_3$, the field of the coexistence opening towards higher temperature with pressure (Tao et al., 2014). A monoclinic phase (dolomite-II) set in driven by rotation of $[CO_3]^{2-}$ groups at 14–20 GPa under ambient temperature (Santillán et al., 2003; Merlini et al., 2019; Stekiel et al., 2019). This new phase was expected to enhance the thermodynamic

stability of (Ca,Mg)CO_3 up to 40 GPa over $MgCO_3$+$CaCO_3$. Above 41 GPa, a triclinic structure (dolomite-III, Z = 8) formed (Merlini et al., 2019).

Naturally Fe^{2+} substitutes Mg^{2+} in dolomite with various contents. Incorporation of Fe^{2+} strongly decreased the order degree of the structure (Tao et al., 2014) and helprf maintain its stability to higher pressures and temperatures (Stekiel et al., 2019). A trigonal → orthorhombic transformation was firstly observed in $(Ca,Mg)_{1.9}Fe_{0.1}(CO_3)_2$ at ~17 GPa and 300 K (Mao et al., 2011). This new orthorhombic phase persisted in upon laser-heating to ~1600–1700 K at 27–31 GPa. At 36–83 GPa, it further transformed to a monoclinic structure. The pressure-induced spin transition of Fe^{2+} was manifested by a drop in the unit-cell volume at ~47 GPa. This observation, however, was not reproduced in Fe-richer counterparts. A similar experimental study on a Fe^{2+}-richer crystal $CaMg_{0.6}Fe_{0.4}(CO_3)_2$, suggested formation of two triclinic structures under pressures (Merlini et al., 2012). One was Fe-dolomite-II (*P*-1; Z = 4), a distortion of the dolomite structure associated by rotation of $[CO_3]^{2-}$ groups, existing between 17 and 35 GPa. The coordination number of Ca^{2+} increased from six in Fe-dolomite to eight in Fe-dolomite-II. The other was Fe-dolomite-III that adopted the same *P*-1 symmetry but had eight formula units in the primitive cell. It exhibited structural relations to $CaCO_3$-III, as the $[CO_3]^{2-}$ units are non-planar with carbon partly in four-fold coordination, some of which edge-shared with Ca^{2+} and Fe^{2+} polyhedra. Fe-dolomite-III had a broad stability domain to 43 GPa and the melting point (~2600 K). Its density was demonstrably comparable to that of the mixture $MgCO_3$+$CaCO_3$ if taking into account the $FeCO_3$ component. The second-order transformation from Fe-dolomite to Fe-dolomite-II was similar to that of dolomite → dolomite-II, and it had been strongly confirmed by Merlini et al. (2019). But above 36 GPa, Merlini et al. (2019) suggested a first-order transition to a rhombohedral symmetry (*R*3) (Fe-dolomite-IIIb). In the pressure range of 70–120 GPa and at 2500 K, Fe-dolomite-IV with an orthorhombic symmetry (*Pnma*) formed. It was charactered with corner-sharing $[CO_4]^{4-}$ units in three-fold rings, similar to $MgCO_3$-*C*2/*m* (Oganov et al., 2008). Different Fe^{2+} contents could be responsible for the disagreement. Previously, Solomatova and Asimow (2016) predicted a monoclinic phase *C*2/*c*as the stable structure for more Fe^{2+}-enriched samples $Ca(Mg_{0.5},Fe_{0.5})(CO_3)_2$ and $CaFe(CO_3)_2$ up to 60 GPa. The *C*2/*c* phase cannot be achieved experimentally due to the large energy barrier and the correspondingly large volume collapse, resulting in conversion from dolomite to metastable structures.

Existing data has revealed the high-pressure behaviors of dolomite, as is summarized in **Figure 1**, but it is limited to draw a full understanding of the structural evolution of Fe-dolomite at pressures and temperatures. Issues deserve evaluation with respect to the effect of Fe^{2+}-content and its spin transition on the thermal and elastic properties and the stability fields (Tao et al., 2014; Merlini et al., 2016), and possibility of energetically competitive structures. Besides, there remains a large area uncovered for pressures above ~60 GPa. We now reach agreements on *1*) a minor addition of Fe^{2+} stabilizes the rhombohedral structure of dolomite against decomposition and transformation under upper mantle conditions; *2*) there stands a good chance for fine changes occurring at ~17 and ~35 GPa, and a decrease trend of crystal symmetry is expected with pressure.

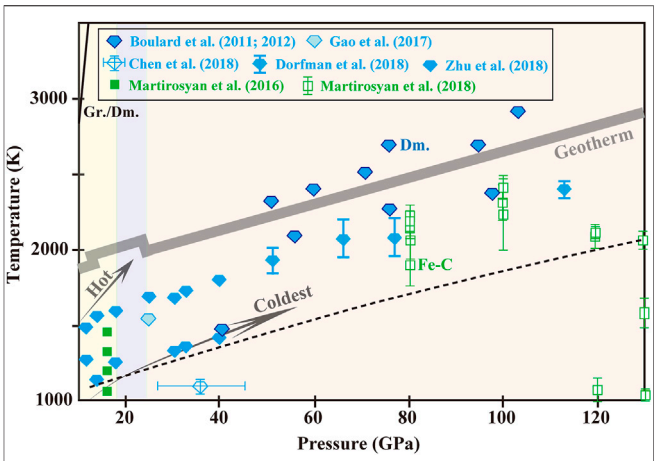

FIGURE 2 | Experimental pressure-temperature conditions and run products of carbonates-Fe^0 system. Blue diamond and green square represent formation of diamond (Dm.) and iron carbide (Fe-C), respectively, with uncertainties estimated for conditions marked. Diamond formation is always along with graphite generation. The dashed black curve is extrapolated from Zhu et al. (2018) for indicating the onset boundary of $MgCO_3$-Fe^0 interaction.

CARBONATES REDUCTION BY REDUCED MANTLE

Given most subduction geotherms, $CaCO_3$, $MgCO_3$, (Ca,Mg)CO_3 and their ferrous series maintain solid polymorphs over a wide range of depths down to the CMB. But their presence in the mantle depends highly as well on oxygen fugacity, which is controlled by oxidation state of iron in minerals and melts (e.g. sulfides and silicates) (Bataleva et al., 2017). A large part of the mantle below 250 km is thought to be Fe^0-sufficient and favorable for reductions of carbonates or carbonatitic melts, which is a potential barrier to carbonates further-subduction and a promising mechanism for sublithospheric diamond formation (Rohrbach and Schmidt, 2011; Stagno et al., 2011). Several carbon species uncovered from the lower-mantle diamonds, vary from oxidized phases (e.g. carbonates) to the reduced (e.g. methane, graphite and iron carbide) (Brenker et al., 2007; Kaminsky and Wirth, 2011; Kaminsky, 2012; Kaminsky et al., 2013, 2016; Smith et al., 2016). That strongly indicates that the redox reactions between subducted carbonates (oxidized) and metallic mantle (reduced) is responsible for sublithospheric diamond genesis (**Figure 2**).

Several studies have been conducted in petrologic context of subducted carbonate assemblages in contact with metallic mantle. One representative study (Palyanov et al., 2013) at 6.5–7.5 GPa and 1273–1873 K documented that $(Mg_{0.9}Ca_{0.1})CO_3$-Fe^0 interaction generated carbonatitic melts, magnesiowustite

(Mg,Fe)O, cohenite Fe_3C and metastable graphite. Increasing temperature led to a higher degree of partial melting but a decrease in Ca^{2+}-component in carbonate melt. Diamonds nucleation from carbonatitic melts (≥1673 K) was expected with heavier carbon isotope relative to the initial carbonate and high concentrations of nitrogen (1000–1500 ppm). In contrast, at iron front where carbide (Fe-C) melt formed, diamond crystallized with lower $\delta^{13}C$ value and only 100–200 ppm of nitrogen mostly in the form of single substitutional aggregation. These chemical characters are analogous to that of natural sublithospheric diamonds. Besides, the accompanying products, iron carbide, graphite and (Mg,Fe)O are characteristic inclusions in natural stones. For simplicity, at the topmost of the upper mantle, $MgCO_3$ reduction by Fe^0 is described as:

$$MgCO_3\,(\text{magnesite}) + Fe^0\,(\text{metal}) \rightarrow (Mg,Fe)O + Fe_3C + C\,(\text{diamond}) \quad (R3-1)$$

Thermodynamic calculations showed that over the entire mantle pressure range, C+(Mg,Fe)O is more stable than $MgCO_3$+Fe-C. Thus, presence of residual carbides in the run products is due to incomplete reaction. A similar experimental work (Martirosyan et al., 2015) later reproduced this observation but for only formation of graphite rather than diamond. That can be accounted for by kinetic impeding for graphite-to-diamond conversion. Increase of temperature and addition of catalysts are two effective methods for diamond formation (Tomlinson et al., 2011; Palyanov et al., 2013).

At higher pressure-temperature conditions, the onset boundary of $MgCO_3$-Fe^0 interaction was defined linearly crossing 1100 K at ~14 GPa and 1375 K at ~40 GPa. The onset of the reaction and diamond nucleation seemed to have nothing to do with partial melting of Fe-C, whichrequired much higher temperatures (Morard et al., 2017). Crystallization of diamond slowed down drastically in 14–18 GPa, corresponding to the mantle depths of 410–525 km (Zhu et al., 2018). That implied a high-pressure kinetic for the reaction and accordingly, a huge reduction in diamond production at the transition zone. The mechanism of the high-pressure kinetic was unknown but it provided a plausible explanation for the abundance of sublithospheric diamond at 250–450 km in contrast to the rarity below. In a broader pressure-temperature range of 70–150 GPa and 1500–2600 K, $MgCO_3$-Fe^0 interaction was exemplified by (Martirosyan et al., 2018):

$$MgCO_3\,(\text{magnesite}) + Fe\,(\text{metal}) \rightarrow FeO + (Mg,Fe)O + Fe_7C_3 + C\,(\text{diamond}) \quad (R3-2)$$

Transformation from $MgCO_3$-*R*-3*c* to *C*2/*m* around 80 GPa exerted little effect on the reaction path. Diamonds nucleated and grew directly from carbonates at subsolidus conditions. Coexistence of FeO+(Mg,Fe)O in the run products suggested an immiscibility gap in MgO-FeO system (Dorfman et al., 2018; Martirosyan et al., 2018). Naturally for worldwide sublithospheric diamonds, (Mg,Fe)O solid solution is the dominant (50–56%) lower-mantle inclusions which presents a broad range in magnesium index ($Mg\# = Mg/(Mg+Fe)_{at.}$, 0.36–0.90). Brazil, the most productive for population of transition zone and lower mantle diamonds, however, possesses (Mg,Fe)O of severely Fe^{2+}-rich, up to $Mg\# = 0.36$ (Kaminsky, 2012). An origin from the D″ layer was proposed as a mechanism to explain this discrepancy (Kaminsky and Wirth, 2011), but it seemed at odds with the immiscibility gap in MgO-FeO system. Factors such as temperature (Palyanov et al., 2013) and oxygen fugacity (Martirosyan et al., 2015) may be more possible to account for the variations of (Mg,Fe)O composition.

In comparison with $MgCO_3$, $CaCO_3$ reacting with Fe^0 proceeded much slower. For $CaCO_3$-Fe^0 coupling in closed systems, Ca-wüstites were identified after reactions at 3–5.5 GPa and 1573–1673 K (5–48 h) with solid carbon in the form of graphite (Chepurov et al., 2011). Similarly for deeper subduction geotherms, interaction of $CaCO_3$-Fe^0 system at 4–16 GPa and 923–1673 K was established as (Martirosyan et al., 2016):

$$CaCO_3\,(\text{aragonite}) + Fe^0\,(\text{metal}) \rightarrow Fe_7C_3 + CaFe_2O_3\,(\text{Ca}-\text{wűstite}) \quad (R3-3)$$

The sluggish kinetics of established $CaCO_3$-Fe^0 interaction suggested that significant amount of carbonates could survive and sink to the transition zone (Martirosyan et al., a 2016). At 6 GPa and 1273–1473 K, redox reaction between $CaCO_3$+$MgCO_3$ mixture and metallic iron resulted in formation of Ca-(Mg,Fe)O and Fe_3C (Martirosyan et al., 2015). But under higher pressure-temperature conditions of 51–113 GPa and 1800–2500 K, the $CaCO_3$ component in $(Mg_{0.38}Ca_{0.59}Fe_{0.03})CO_3$ seemed unresponsive in the reactions but remained in the phase of post-aragonite (Dorfman et al., 2018). Model of carbonates-Fe^0 interaction was applicable to Fe^{2+}-carbonates self-reduction, where Fe^{2+} disproportionated and reacted with C^{4+} to form diamond and Fe^{3+}-oxides at lower mantle pressures (*see* **Section 2.2**; Boulard et al., 2011; 2012; 2015; Chen et al., 2018). But diamonds nucleated from Fe^{2+}-carbonates self-reduction were too tiny to be analyzed.

For all the carbon-phases during carbonates-Fe^0 interaction, a closer look leads us to check the behaviors of iron carbide (e.g. cohenite Fe_3C, Fe_7C_3). Iron carbide has been discovered as inclusions in sublithospheric diamonds (Kaminsky and Wirth, 2011) and silicates which are believed to originate at various depths spanning from the upper mantle to possibly the CMB. That indicates an active participation of iron carbide in deep carbon cycle. Iron carbides could form by solid-solid reaction in portions of the Earth's interior where metallic iron and elemental carbon or carbonateare in mutual contact (Palyanov et al., 2013). It dissolves carbon with bulk content as high as ~300 ppm, and maintains stable in the reduced mantle environments with oxygen fugacity values close to or below IW buffer equilibrium. Besides, multiple lines of evidence suggest a mantle with sulfide-rich metallic melt (Stachel and Harris, 2008; Zhang Z. et al., 2018). Owing to strong non-ideal mixing between carbon and sulfur in Fe-bearing alloy, the

presence of sulfur significantly lower the solubility of carbon and trigger carbon exsolution from the carbide (Zhang Z. et al., 2018). The discovery of a carbide+sulfide+metal assemblage in sublithospheric diamonds shed lights on mechanism of diamond formation from Fe-C-S melt (Smith et al., 2016). Here we evaluate the phase relations of Fe-C-S systems in the mantle focusing on exsolution of diamond. Chemical reactions involving:

$$2Fe_3C + 3S_2 \rightarrow 6FeS + 2C^0 \quad (R3-4)$$

$$Fe_3C + 3FeS_2 \rightarrow 6FeS + C^0 \quad (R3-5)$$

Most studies on Fe-C-S systems were performed at pressures ≤8 GPa (Bataleva et al., 2017). These studies reported efficient capabilities of Fe_3C to generate graphite (1473–1873 K), diamond (1573–1873 K) and pyrrhotite (FeS) in the presence of sulfur-bearing metasomatic agents; further temperature increase led to higher efficiency of diamond crystallization. The established Fe-C-S model was applicable to Fe-Ni-C-S system, where Fe-Ni alloy showed a greater accommodation of dissolved carbon with temperature up to 2600 K but at lower pressures (≤20 GPa) (Narygina et al., 2011).

Redox reactions between subducted carbonates and Fe^{2+}-peridotites/eclogites can be taken as a simplified model of slab-mantle interactions processing in the deep zones. It was mainly controlled by low concentrations of carbonates and metallic iron at the CMB as well as low diffusion of chemical components (e.g. O^{2-}, Fe^{2+}) among silicates and carbonates. This is a limited process and set constraints for carbon speciation and protections for carbonates from reduction (**Figure 2**). Likely that a significant amount of (Ca,Mg,Fe)-carbonates may survive from Fe^0-saturation boundary (Martirosyan et al., a 2016) at the upper mantle and the transition zone. But at the top of the lower mantle due to stagnation of subducting slabs, carbonates accumulate and are heated up. Carbonates-Fe^0 interaction would be more probable for diamond production. The rate of graphite-to-diamond transformation was higher in a FeNi system. Higher pressure appeared to favor growth of cubo-octahedral diamonds, whereas octahedral diamonds grow at lower pressure conditions (≤10 GPa in $MgCO_3$ and ≤15 GPa in FeNi). The run products lacked the slip planes and lamination lines commonly associated with superdeep diamonds, and we may suggest that these deformation features are due to transport instead of growth conditions (Tomlinson et al., 2011). Accompanying with carbon freezing in the Earth, carbon isotope fractionation occurs. The carbon isotope composition in the mantle displays a well-defined peak around $\delta^{13}C = -5‰$ in an extensive range to the lowest of ~−40‰. Subduction of organic carbon was advocated for the mantle regions with ^{13}C depletion. Relatively, reduction of carbonates extracted ^{12}C to a greater degree and it was more likely to contribute to the broad distribution of carbon in the mantle (Horita and Polyakov, 2015).

CARBONATES DECARBONIZATION BY SILICATES

In consideration of major minerals in basaltic plates and the mantle, carbonate stability should also be inspected by carbonates-silicates interactions under mantle conditions. This reaction sets fundamental control not merely on subduction limit of carbonate or CO_2 release in the mantle, but on physicochemical properties of the mantle such as initiation of melting by lowering the mantle solidus, generation of alkalic magma in oceanic islands and carbonate metasomatism in cratonic mantle. Two typical chemical reactions are appraised here:

$$CaCO_3 + SiO_2 \rightarrow CaSiO_3 + CO_2 \quad (R4-1)$$

$$MgCO_3 + SiO_2 \rightarrow MgSiO_3 + CO_2 \quad (R4-2)$$

SiO_2 is one of the abundant components in MORB. Along subduction geotherms, SiO_2 changes to its high-pressure polymorphs as coesite, stishovite, $CaCl_2$-type and seifertite successively (Murakami et al., 2003; Grocholski et al., 2013). According to experimental and theoretical results, even for the temperature profiles in cold subduction slabs, $CaCO_3$-VII reacted with SiO_2-stishovite above 23 GPa and 1500 K to produce $CaSiO_3$-perovskite and possibly free CO_2. High temperature greatly increased the tendency of partitioning Ca^{2+} from carbonates $CaCO_3$ to silicates $CaSiO_3$ (Zhang ZG. et al., 2018; Li et al., 2018), accounting for the observation of abundance of $CaSiO_3$-perovskite in sublithospheric diamonds compared to typical mantle mineralogy. Decarbonation of $MgCO_3$ by SiO_2-coesite was confirmed beginning at 6–7 GPa and above 1600 K, and the decarbonatation temperature increased sharply with pressure (Palyanov et al., 2002; Kakizawa et al., 2015). An addition of alkali-component to $MgCO_3$-SiO_2 system negligibly changed the reaction path, and the output diamond was close to the initial $MgCO_3$ in terms of carbon isotopic composition (Palyanov et al., 2002). At 28–62 GPa and 1490–2000 K (770–1500 km), $MgSiO_3$-perovskite and solid CO_2 (V or VI) formed from interactions between $MgCO_3$ and SiO_2-stishovite (Takafuji et al., 2006). With this regard, both $CaCO_3$ and $MgCO_3$ was unstable and would release CO_2 to the lower mantle for SiO_2-rich subducted basalts.

Calculations carried out at higher pressures of 50–200 GPa under static conditions (0 K) showed that $CaCO_3$ (post-aragonite) and $MgCO_3$ (*R*-3*c*) maintained stable but react with SiO_2 at closely the CMB (Oganov et al., 2008; Pickard and Needs, 2015; Santos et al., 2019). This was contradictory to the experimental observations (Maeda et al., 2017) where the reaction of $MgCO_3$-SiO_2 occurred at mantle depth beginning from ~1000 km and that held true for all the mantle regions below. Different results could be due to different conditions in these studies. $MgCO_3$-*R*-3*c* reacted with SiO_2-stishovite for formation of $MgSiO_3$-bridgmanite and CO_2-VI (six-fold coordinated of carbon) at depths around 1700 km (83 GPa; 1780 K). Internal production of CO_2 from $MgCO_3$-SiO_2 system was thus, possible in the middle of the lower mantle (1700–1900 km) and at greater depths CO_2-VI would decompose

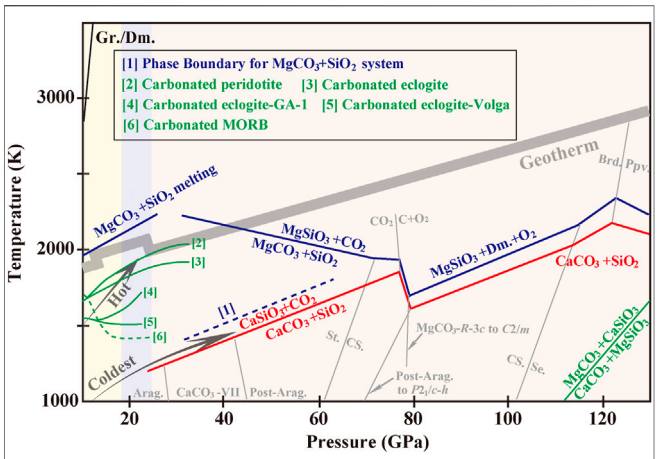

FIGURE 3 | Schematic reaction line of carbonate-silicate at the Earth's mantle conditions. The black lines representing $CaCO_3$-SiO_2 reaction is measured according to Li et al. (2018) and Zhang and Liu (2015). The dark-blue lines indicate phase boundaries for $MgCO_3$-SiO_2 system (solid: Maeda et al., 2017; dotted [1]: Takafuji et al., 2006). Partial melting of $MgCO_3$-SiO_2 series produces a simple eutectic system (Kakizawa et al., 2015). Curve [2] represents solidus curve of carbonated peridotite (Litasov and Ohtani, 2009). Solidus curves of carbonated eclogites are plotted according to Litasov and Ohtani (2010) (Curve [3]) and Kiseeva et al. (2013) (Curve [4], [5]). The melting curve of carbonated MORB (Curve [6]) according to Thomson et al. (2016). Phase diagram for the stability of $MgCO_3$+$CaSiO_3$ versus $CaCO_3$+$MgSiO_3$ is referred to Santos et al. (2019). Phase boundaries of $CaCO_3$- and $MgCO_3$-polymorphs follow the references in **Section 2.1**. The phase diagrams of SiO_2 (Murakami et al., 2003; Grocholski et al., 2013), CO_2 (Litasov et al., 2011) and $MgSiO_3$ (Komabayashi et al., 2008) are included with gray solid lines. Abbreviations: Gr., graphite; Dm., diamond; St., stishovite; CS., $CaCl_2$-type SiO_2; Se., seifertite; Brd., $MgSiO_3$ bridgmanite; Ppv., $MgSiO_3$ post-perovskite.

to diamond. If survived, $MgCO_3$-*R*-3*c* changed to *C*2/*m* and reacted with SiO_2-seifertite to generate $MgSiO_3$-post-perovskite and diamond at the lowermost mantle.

Figure 3 summarizes the phase relations of carbonate-silicate system at mantle conditions. The solidus of the carbonated MORB intersected most subduction geotherms at mantle depths of 300–700 km, creating a focused region of melt at the top of the transition zone and producing a barrier to carbonate recycling into the deep mantle (Thomson et al., 2016). But in super-cold slabs, carbonated MORB would survive from the melting process and sink further. Carbonation reactions involving olivine or pyroxene tended to react with CO_2 to form carbonate without dissociation into a CO_2-bearing assemblage, so present-day subduction of oceanic crust likely introduced carbon into the mantle in the form of carbonated eclogite. Phase relations of CaO-MgO-Al_2O_3-SiO_2-CO_2 system exhibited a substantial increase in $MgCO_3$ component in melt compositions from lower pressures (12–16 GPa) to the higher (20–25 GPa). That may be due to $CaSiO_3$-perovskite formation at 20 GPa but $MgSiO_3$-perovskite required higher pressures (Keshav and Gudfinnsson, 2010). For carbonates with high bulk alkali contents, the alkali-rich carbonates tended to form a solid solution with Ca^{2+} but left Mg^{2+} incorporating into majorite. What is striking was that most carbon in SiO_2-rich melts partitioned into alkali-rich aragonite and diamond, whereas little diamond formed in SiO_2-deficient melts. It may be accounted for by more progressive Fe^{2+}-Fe^{3+} transformation with pressure in SiO_2-rich melts (Kiseeva et al., 2013). Along subduction geotherms from the upper mantle to the transition zone, carbon-phases in alkali-rich carbonated eclogites evolve following the route of "$MgCO_3$+$CaCO_3$ (aragonite) or $MgCO_3$-$CaCO_3$ (calcite) solid solution → $MgCO_3$+alkali-rich $CaCO_3$ (aragonite) → alkali-rich $CaCO_3$ (aragonite) → graphite and diamond."

$$CaCO_3 + MgO \rightarrow CaO + MgCO_3 \quad (R4-3)$$

$$CaCO_3 + MgSiO_3 \rightarrow CaSiO_3 + MgCO_3 \quad (R4-4)$$

Calculations indicated that the reaction R4-3 was energetically unfavorable over the entire mantle. That is, $CaCO_3$ is stable under thermodynamic conditions if there is MgO in excess as expected in a pyrolitic mantle (Oganov et al., 2008; Pickard and Needs, 2015; Santos et al., 2019). For the conditions of $MgSiO_3$ in excess (R4-4), which was the main mineral in the lower mantle, $CaCO_3$ would be consumed and the $MgCO_3$+$CaSiO_3$ association was more favorable to the mid-mantle, hereafter $CaCO_3$ became restabilized over $MgCO_3$ (Oganov et al., 2008; Pickard and Needs, 2015; Zhang ZG. et al., 2018; Santos et al., 2019). The higher densities of the $CaCO_3$-polymorphs relative to the $MgCO_3$-polymorphs could be responsible for the free energy change of the reaction. However, temperature and chemical potentials need to be taken into account further as they can shift the phase relations conceivably. Santos et al. (2019) believed that an increase in temperature increased the pressure at which the reaction becomes unfavorable. That is, $MgCO_3$ was the main host of oxidized carbon over almost the mantle. But for super-cold subduction geotherms, $CaCO_3$ was more stable than $MgCO_3$.

As is highlighted in **Figure 3**, during deep-subduction processes, $MgCO_3$ exhibits much higher stability relative to $CaCO_3$ in consideration of existence of subducted SiO_2 and $MgSiO_3$ in a pyrolitic mantle model. Only for locally regions where MgO is in excess, $CaCO_3$ could be preserved to the CMB. Carbonatitic melts reacting with SiO_2 would release CO_2 (solid) into the lower mantle, which will eventually decompose to diamond.

CONCLUSIONS AND PROSPECTS

Carbonates play a key role in the recycling of carbon from the Earth's crust to the interior *via* subduction processes, producing one of the carbon budgets in the entire Earth's system. In light of the striking discoveries above, we now have a much clearer picture of behaviors of carbonates in the deep Earth.

First, several new polymorphs have been identified as stable of $CaCO_3$, $MgCO_3$ and $(Ca,Mg)CO_3$ and their ferrous series (**Figure 1**), which improve our expectations for their possibilities in the mantle. Existence of carbonates and the occurrence of the phase transitions may correlate with the discontinuities in the Earth's seismic profile. Carbonates of $CaCO_3$-$MgCO_3$-$FeCO_3$ series remain in solid phases along

most modern subduction geotherms. So liberation of carbonatitic melts or CO_2 owing to carbonate decomposition seems unlikely, with such possibility restricted merely for conditions in hot zones. However, decarbonization of $CaCO_3$ and $MgCO_3$ takes place in SiO_2-rich subducted basalts under the lower-mantle conditions (**Figure 3**). CO_2 decomposing to diamond is energetically favored in the region from the middle of the lower mantle to the CMB. Meanwhile, carbonates in slabs tend to be reduced to diamond at metal-saturation boundary at the topmost of the lower mantle (**Figure 2**). Diamonds produced from slab-mantle interactions are similar to natural stones in terms of chemical composition and inclusion characteristics. So far the existing data have covered almost the entire mantle conditions for decarbonization and reduction of carbonates and documented diamond nucleation. In this regard, carbonates reduction and decarbonization are effective mechanisms of carbon sequestration at the top-mid region of the lower mantle.

Researches on carbon cycle throughout the Earth's system have long represented an interesting frontier. One fundamental goal of carbon cycle research is to know the balance between income and outcome global carbon fluxes as well as the carbon fluxes change in space and time. But many details of the processes remain unclear for the lack of intensive monitoring. Three issues may be worth of particular considerations in the future work:

(1) Besides carbonates, CO_2 and iron carbides mentioned above, there could exist other chemical forms of carbon in the mantle that has been uncovered, for example, a new carbon phase of $Fe_4(CO_4)_3$ derived from decomposition of Fe-bearing carbonates (Boulard et al., 2015). So a critical and pressing task is to search for these undiscovered carbon. Given the scarcity of natural samples, we may gain insights by thermodynamic calculations and experiments. These efforts will shed new lights on our view on deep carbon reservoirs, for example, how they form and under what conditions are they stable for long.
(2) Existing experiments have confirmed the possibility of redox reactions between subducted carbonates and metallic mantle to produce sublithospheric diamonds and other reduced carbon species. However, it is not yet clear whether carbonates-Fe^0 processes generate significant amounts of diamonds. To what extent do carbonates turn into diamonds? And what role has the remaining carbonatitic melts played in deep carbon cycle and besides, in mantle metasomatism. These questions are basically related to the kinetics of carbonates-Fe^0 interactions that set constraints on sequestration efficiency directly of deep carbon. Besides, carbon isotope fractionation during slab-mantle interactions is also an essential part in the study of deep carbon cycle. However, previous insights have been gained from theoretical calculations (Horita and Polyakov, 2015), as natural samples are too scarce. Experiments conducted at high-pressure and high-temperature conditions may be a favor to synthesize large samples.
(3) Now we have a better knowledge of carbon recycle in the carbonated MORB during deep subduction processes. Yet there is an increasing recognition that continental crust carrying sedimentary carbonate rocks can subduct to the upper mantle (Zhu et al., 2009). With depth, a certain amount of CO_2 is released from carbonatitic components *via* progressive metamorphism. Moreover, higher metamorphic temperatures enhance the activity of fluids in subduction zones, which significantly promotes decarbonization of carbonates (Zhang ZG. et al., 2018; Li et al., 2018). We believe that such reactions are a widespread process and exert an assignable effect upon carbon flux between the Earth's surface and the interior. So equally important are efforts to be made on processes and rates by which carbon cycle in continental subduction zones.

AUTHOR CONTRIBUTIONS

JG wrote the original draft. XW, XY, and WS were responsible for the review and modification.

ACKNOWLEDGMENTS

The authors are thankful to the reviewers.

REFERENCES

Antao, S. M., and Hassan, I. (2009). The Orthorhombic Structure of CaCO3, SrCO3, PbCO3 and BaCO3: Linear Structural Trends. *Can. Mineral.* 47 (5), 1245–1255. doi:10.3749/canmin.47.5.1245

Bataleva, Y. V., Palyanov, Y. N., Borzdov, Y. M., Bayukov, O. A., and Zdrokov, E. V. (2017). Iron Carbide as a Source of Carbon for Graphite and Diamond Formation Under Lithospheric Mantle P-T Parameters. *Lithos* 286-287, 151–161. doi:10.1016/j.lithos.2017.06.010

Bayarjargal, L., Fruhner, C.-J., Schrodt, N., and Winkler, B. (2018). CaCO3 Phase Diagram Studied with Raman Spectroscopy at Pressures up to 50 GPa and High Temperatures and DFT Modeling. *Phys. Earth Planet. Interiors* 281, 31–45. doi:10.1016/j.pepi.2018.05.002

Bayarjargal, L., Shumilova, T. G., Friedrich, A., and Winkler, B. (2010). Diamond Formation from CaCO3 at High Pressure and Temperature. *ejm* 22, 29–34. doi:10.1127/0935-1221/2010/0021-1986

Boulard, E., Menguy, N., Auzende, A. L., Benzerara, K., Bureau, H., Antonangeli, D., et al. (2012). Experimental Investigation of the Stability of Fe-Rich Carbonates in the Lower Mantle. *J. Geophys. Res.* 117, B02208. doi:10.1029/2011jb008733

Boulard, E., Gloter, A., Corgne, A., Antonangeli, D., Auzende, A.-L., Perrillat, J.-P., et al. (2011). New Host for Carbon in the Deep Earth. *Proc. Natl. Acad. Sci.* 108 (13), 5184–5187. doi:10.1073/pnas.1016934108

Boulard, E., Pan, D., Galli, G., Liu, Z., and Mao, W. L. (2015). Tetrahedrally Coordinated Carbonates in Earth's Lower Mantle. *Nat. Commun.* 6, 6311. doi:10.1038/ncomms7311

Brenker, F. E., Vollmer, C., Vincze, L., Vekemans, B., Szymanski, A., Janssens, K., et al. (2007). Carbonates from the Lower Part of Transition Zone or Even the Lower Mantle. *Earth Planet. Sci. Lett.* 260, 1–9. doi:10.1016/j.epsl.2007.02.038

Bundy, F. P., Bassett, W. A., Weathers, M. S., Hemley, R. J., Mao, H. U., and Goncharov, A. F. (1996). The Pressure-Temperature Phase and Transformation Diagram for Carbon; Updated Through 1994. *Carbon* 34, 141–153. doi:10.1016/0008-6223(96)00170-4

Chen, M., Shu, J., Xie, X., Tan, D., and Mao, H.-k. (2018). Natural Diamond Formation by Self-Redox of Ferromagnesian Carbonate. *Proc. Natl. Acad. Sci. USA* 115 (11), 2676–2680. doi:10.1073/pnas.1720619115

Chepurov, A. I., Sonin, V. M., Zhimulev, E. I., Chepurov, A. A., and Tomilenko, A. A. (2011). On the Formation of 621 Element Carbon During Decomposition of CaCO3 at High P-T Parameters Under Reducing Conditions. *622 Doklady Earth Sciences* 441 (2), 1738–1741.

Dasgupta, R., and Hirschmann, M. M. (2010). The Deep 623 Carbon Cycle and Melting in Earth's Interior. *Earth Planet. Sci. Lett.* 298, 1–13.

Dorfman, S. M., Badro, J., Nabiei, F., Prakapenka, V. B., Cantoni, M., and Gillet, P. (2018). Carbonate Stability in the Reduced Lower Mantle. *Earth Planet. Sci. Lett.* 489, 84–91. doi:10.1016/j.epsl.2018.02.035

Farsang, S., Louvel, M., Zhao, C. S., Mezouar, M., Rosa, A. D., Widmer, R. N., et al. (2021). Deep Carbon Cycle Constrained by Carbonate Solubility. *Nature Communications* 12, 4311.

Frost, D. J., Liebske, C., Langenhorst, F., McCammon, C. A., Trønnes, R. G., and Rubie, D. C. (2004). Experimental Evidence for the Existence of Iron-Rich Metal in the Earth's Lower Mantle. *Nature* 428, 409–412. doi:10.1038/nature02413

Fu, S., Yang, J., and Lin, J. F. (2017). Abnormal Elasticity of Single-Crystal Magnesiosiderite Across the Spin Transition in Earth's Lower Mantle. *Phys. Rev. Lett.* 118, 036402. doi:10.1103/PhysRevLett.118.036402

Gavryushkin, P. N., Martirosyan, N. S., Inerbaev, T. M., Popov, Z. I., Rashchenko, S. V., Likhacheva, A. Y., et al. (2017). Aragonite-II and CaCO3-VII: New High-Pressure, High-Temperature Polymorphs of CaCO3. *Cryst. Growth Des.* 17, 6291–6296. doi:10.1021/acs.cgd.7b00977

Ghosh, S., Ohtani, E., Litasov, K. D., and Terasaki, H. (2009). Solidus of Carbonated Peridotite from 10 to 20 GPa and Origin of Magnesiocarbonatite Melt in the Earth's Deep Mantle. *Chem. Geology.* 262, 17–28. doi:10.1016/j.chemgeo.2008.12.030

Gorman, P. J., Kerrick, D. M., and Connolly, J. A. D. (2006). Modeling Open System Metamorphic Decarbonation of Subducting Slabs. *Geochem. Geophys. Geosystems* 7 (4), Q04007. doi:10.1029/2005gc001125

Grocholski, B., Shim, S.-H., and Prakapenka, V. B. (2013). Stability, Metastability, and Elastic Properties of a Dense Silica Polymorph, Seifertite. *J. Geophys. Res. Solid Earth* 118, 4745–4757. doi:10.1002/jgrb.50360

Hammouda, T., Chantel, J., Manthilake, G., Guignard, J., and Crichton, W. (2015). Hot Mantle Geotherms Stabilize Calcic Carbonatite Magmas up to the Surface. *Geology* 42, 911–914. doi:10.1130/G35778.1

Horita, J., and Polyakov, V. B. (2015). Carbon-bearing Iron Phases and the Carbon Isotope Composition of the Deep Earth. *Proc. Natl. Acad. Sci. USA* 112 (1), 31–36. doi:10.1073/pnas.1401782112

Hsu, H., and Huang, S-C. (2016). Spin Crossover and Hyperfine Interactions of Iron in $(Mg,Fe)CO_3$ Ferromagnesite. *Phys. Rev. B* 94, 060404. doi:10.1103/physrevb.94.060404

Huang, D., Liu, H., Hou, M.-Q., Xie, M.-Y., Lu, Y.-F., Liu, L., et al. (2017). Elastic Properties of CaCO 3 High Pressure Phases from First Principles. *Chin. Phys. B* 26 (8), 089101. doi:10.1088/1674-1056/26/8/089101

Irving, A. J., and Wyllie, P. J. (1975). Subsolidus and Melting Relationships for Calcite, Magnesite and the Join CaCO3-MgCO3 36 Kb. *Geochimica et Cosmochimica Acta* 39 (1), 35–53. doi:10.1016/0016-7037(75)90183-0

Isshiki, M., Irifune, T., Hirose, K., Ono, S., Ohishi, Y., Watanuki, T., et al. (2004). Stability of Magnesite and its High-Pressure Form in the Lowermost Mantle. *Nature* 427, 60–63. doi:10.1038/nature02181

Johnston, F. K. B., Turchyn, A. V., and Edmonds, M. (2011). Decarbonation Efficiency in Subduction Zones: Implications for Warm Cretaceous Climates. *Earth Planet. Sci. Lett.* 303, 143–152. doi:10.1016/j.epsl.2010.12.049

Kakizawa, S., Inoue, T., Suenami, H., and Kikegawa, T. (2015). Decarbonation and Melting in MgCO3-SiO2 System at High Temperature and High Pressure. *J. Mineralogical Petrological Sci.* 110, 179–188. doi:10.2465/jmps.150124

Kaminsky, F. (2012). Mineralogy of the Lower Mantle: A Review of 'super-Deep' mineral Inclusions in Diamond. *Earth-Science Rev.* 110, 127–147. doi:10.1016/j.earscirev.2011.10.005

Kaminsky, F. V., Ryabchikov, I. D., and Wirth, R. (2016). A Primary Natrocarbonatitic Association in the Deep Earth. *Miner Petrol.* 110, 387–398. doi:10.1007/s00710-015-0368-4

Kaminsky, F. V., and Wirth, R. (2011). Iron Carbide Inclusions in Lower-Mantle diamond from Juina, Brazil. *Can. Mineral.* 49, 555–572. doi:10.3749/canmin.49.2.555

Kaminsky, F. V., Wirth, R., and Schreiber, A. (2013). Carbonatitic Inclusions in Deep Mantle diamond from Juina, Brazil: New Minerals in the Carbonate-Halide Association. *Can. Mineral.* 51, 669–688. doi:10.3749/canmin.51.5.669

Kaneshima, S. (2013). Lower Mantle Seismic Scatterers below the Subducting Tonga Slab: Evidence for Slab Entrainment of Transition Zone Materials. *Phys. Earth Planet. Interiors* 222, 35–46. doi:10.1016/j.pepi.2013.07.001

Kang, N., Schmidt, M. W., Poli, S., Connolly, J. A. D., and Franzolin, E. (2016). Melting Relations in the System FeCO3-MgCO3 and Thermodynamic Modelling of Fe-Mg Carbonate Melts. *Contrib. Mineral. Petrol.* 171, 74. doi:10.1007/s00410-016-1283-3

Kang, N., Schmidt, M. W., Poli, S., Franzolin, E., and Connolly, J. A. D. (2015). Melting of Siderite to 20GPa and Thermodynamic Properties of FeCO3-Melt. *Chem. Geology.* 400, 34–43. doi:10.1016/j.chemgeo.2015.02.005

Katsura, T., Yoneda, A., Yamazaki, D., Yoshino, T., and Ito, E. (2010). Adiabatic Temperature Profile in the Mantle. *Phys. Earth Planet. Interiors* 183, 212–218. doi:10.1016/j.pepi.2010.07.001

Kelemen, P. B., and Manning, C. E. (2015). Reevaluating Carbon Fluxes in Subduction Zones, What Goes Down, Mostly Comes up. *Proc. Natl. Acad. Sci. USA* 112 (30), E3997–E4006. doi:10.1073/pnas.1507889112

Keshav, S., and Gudfinnsson, G. H. (2010). Experimentally Dictated Stability of Carbonated Oceanic Crust to Moderately Great Depths in the Earth: Results from the Solidus Determination in the System CaO-MgO-Al2O3-SiO2-CO2. *J. Geophys. Res.* 115, B05205. doi:10.1029/2009jb006457

Kiseeva, K., Litasov, K. D., Yaxley, G. M., Ohtani, E., and Kamenetsky, V. S. (2013). Melting and Phase Relations of Carbonated Eclogite at 9-21GPa and the Petrogenesis of Alkali-Rich Melts in the Deep Mantle. *J. Petrology* 54, 1–29. doi:10.1093/petrology/egt023

Komabayashi, T., Hirose, K., Sugimura, E., Sata, N., Ohishi, Y., and Dubrovinsky, L. S. (2008). Simultaneous Volume Measurements of Post-perovskite and Perovskite in MgSiO3 and Their Thermal Equations of State. *Earth Planet. Sci. Lett.* 265, 515–524. doi:10.1016/j.epsl.2007.10.036

Li, J., and Yuen, D. A. (2014). Mid-mantle Heterogeneities Associated with Izanagi Plate: Implications for Regional Mantle Viscosity. *Earth Planet. Sci. Lett.* 385, 137–144. doi:10.1016/j.epsl.2013.10.042

Li, X. Y., Zhang, Z. G., Lin, J. F., Ni, H. W., Prakapenka, V. B., and Mao, Z. (2018). New High Pressure Phase of $CaCO_3$ at the Topmost Lower Mantle: Implication for the Deep Mantle Carbon Transportation. *Geophys. Res. Lett.* 45, 1335–1360. doi:10.1002/2017gl076536

Li, Z., Li, J., Lange, R., Liu, J., and Militzer, B. (2017). Determination of Calcium Carbonate and Sodium Carbonate Melting Curves up to Earth's Transition Zone Pressures with Implications for the Deep Carbon Cycle. *Earth Planet. Sci. Lett.* 457, 395–402. doi:10.1016/j.epsl.2016.10.027

Lin, J.-F., Liu, J., Jacobs, C., and Prakapenka, V. B. (2012). Vibrational and Elastic Properties of Ferromagnesite Across the Electronic Spin-Pairing Transition of Iron. *Am. Mineral.* 97, 583–591. doi:10.2138/am.2012.3961

Litasov, K. D., Fei, Y., Ohtani, E., Kuribayashi, T., and Funakoshi, K. (2008). Thermal Equation of State of Magnesite to 32GPa and 2073K. *Phys. Earth Planet. Interiors* 168, 191–203. doi:10.1016/j.pepi.2008.06.018

Litasov, K. D., Goncharov, A. F., and Hemley, R. J. (2011). Crossover from Melting to Dissociation of CO2 Under Pressure: Implications for the Lower Mantle. *Earth Planet. Sci. Lett.* 309, 318–323. doi:10.1016/j.epsl.2011.07.006

Litasov, K. D., Ohtani, E., Ghosh, S., Nishihara, Y., Suzuki, A., and Funakoshi, K. (2007). Thermal Equation of State of Superhydrous Phase B to 27GPa and 1373K. *Phys. Earth Planet. Interiors* 164, 142–160. doi:10.1016/j.pepi.2007.06.003

Litasov, K. D., and Ohtani, E. (2009). Solidus and Phase Relations of Carbonated Peridotite in the System CaO-Al2O3-MgO-SiO2-Na2O-CO2 to the Lower Mantle Depths. *Phys. Earth Planet. Interiors* 177, 46–58. doi:10.1016/j.pepi.2009.07.008

Litasov, K. D., Shatskiy, A., Gavryushkin, P. N., Bekhtenova, A. E., Dorogokupets, P. I., Danilov, B. S., et al. (2017). P-V-T Equation of State of CaCO 3 Aragonite to 29 GPa and 1673 K: In Situ X-ray Diffraction Study. *Phys. Earth Planet. Interiors* 265, 82–91. doi:10.1016/j.pepi.2017.02.006

Litasov, K., and Ohtani, E. (2010). The Solidus of Carbonated Eclogite in the System CaO-Al2O3-MgO-SiO2-Na2O-CO2 to 32GPa and Carbonatite Liquid in the Deep Mantle. *Earth Planet. Sci. Lett.* 295, 115–126. doi:10.1016/j.epsl.2010.03.030

Litvin, Y., Spivak, A., Solopova, N., and Dubrovinsky, L. (2014). On Origin of Lower-Mantle Diamonds and Their Primary Inclusions. *Phys. Earth Planet. Interiors* 228, 176–185. doi:10.1016/j.pepi.2013.12.007

Liu, J., Lin, J.-F., and Prakapenka, V. B. (2015). High-pressure Orthorhombic Ferromagnesite as a Potential Deep-Mantle Carbon Carrier. *Sci. Rep.* 5, 7640. doi:10.1038/srep07640

Lobanov, S. S., Dong, X., Martirosyan, N. S., Samtsevich, A. I., Stevanovic, V., Gavryushkin, P. N., et al. (2017). Raman Spectroscopy and X-ray Diffraction of sp3CaCO3 at Lower Mantle Pressures. *Phys. Rev. B* 96, 104101. doi:10.1103/physrevb.96.104101

Maeda, F., Ohtani, E., Kamada, S., Sakamaki, T., Hirao, N., and Ohishi, Y. (2017). Diamond Formation in the Deep Lower Mantle: A High-Pressure Reaction of MgCO3 and SiO2. *Sci. Rep.* 7, 40602. doi:10.1038/srep40602

Mao, Z., Armentrout, M., Rainey, E., Manning, C. E., Dera, P., Prakapenka, V. B., et al. (2011). Dolomite III: A New Candidate Lower Mantle Carbonate. *Geophys. Res. Lett.* 38, L22303. doi:10.1029/2011gl049519

Marcondes, M. L., Justo, J. F., and Assali, L. V. C. (2016). Carbonates at High Pressures: Possible Carriers for Deep Carbon Reservoirs in the Earth's Lower Mantle. *Phys. Rev. B* 94, 104112. doi:10.1103/physrevb.94.104112

Martirosyan, N. S., Litasov, K. D., Lobanov, S. S., Goncharov, A. F., Shatskiy, A., Ohfuji, H., et al. (2018). The Mg-Carbonate-Fe Interaction: Implication for the Fate of Subducted Carbonates and Formation of Diamond in the Lower Mantle. *Geosci. Front.* 10, 1–10.

Martirosyan, N. S., Litasov, K. D., Shatskiy, A., and Ohtani, E. (2015). The Reactions Between Iron and Magnesite at 6 GPa and 1273-1873 K: Implication to Reduction of Subducted Carbonate in the Deep Mantle. *J. Mineralogical Petrological Sci.* 110, 49–59. doi:10.2465/jmps.141003a

Martirosyan, N. S., Yoshino, T., Shatskiy, A., Chanyshev, A. D., and Litasov, K. D. (2016). The CaCO3-Fe Interaction: Kinetic Approach for Carbonate Subduction to the Deep Earth's Mantle. *Phys. Earth Planet. Interiors* 259, 1–9. doi:10.1016/j.pepi.2016.08.008

Merlini, M., Cerantola, V., Gatta, G. D., Gemmi, M., Hanfland, M., Kupenko, I., et al. (2019). Dolomite-IV: Candidate Structure for a Carbonate in the Earth's Lower Mantle. *Am. Mineral.* 102 (8), 1763–1766. doi:10.2138/am-2017-6161

Merlini, M., Crichton, W. A., Hanfland, M., Gemmi, M., Muller, H., Kupenko, I., et al. (2012). Structures of Dolomite at Ultrahigh Pressure and Their Influence on the Deep Carbon Cycle. *Proc. Natl. Acad. Sci.* 109 (34), 13509–13514. doi:10.1073/pnas.1201336109

Merlini, M., Sapelli, F., Fumagalli, P., Gatta, G. D., Lotti, P., Tumiati, S., et al. (2016). High-temperature and High-Pressure Behavior of Carbonates in the Ternary Diagram CaCO3-MgCO3-FeCO3. *Am. Mineral.* 101, 1423–1430. doi:10.2138/am-2016-5458

Morard, G., Andrault, D., Antonangeli, D., Nakajima, Y., Auzende, A. L., Boulard, E., et al. (2017). Fe-FeO and Fe-Fe3C Melting Relations at Earth's Core-Mantle Boundary Conditions: Implications for a Volatile-Rich or Oxygen-Rich Core. *Earth Planet. Sci. Lett.* 473, 94–103. doi:10.1016/j.epsl.2017.05.024

Murakami, M., Hirose, K., Ono, S., and Ohishi, Y. (2003). Stability of $CaCl_2$-type and PbO_2-type SiO_2 at High Pressure and Temperature Determined by In-Situ X-ray Measurements. *Geophys. Res. Lett.* 30, 1207. doi:10.1029/2002gl016722

Narygina, O., Dubrovinsky, L. S., McCammon, C. A., Kurnosov, A., Kantor, I. Y., Prakapenka, V. B., et al. (2011). X-ray Diffraction and Mössbauer Spectroscopy Study of Fcc Iron Hydride FeH at High Pressures and Implications for the Composition of the Earth's Core. *Earth Planet. Sci. Lett.* 307, 409–414. doi:10.1016/j.epsl.2011.05.015

Niu, F. (2014). Distinct Compositional Thin Layers at Mid-mantle Depths beneath Northeast China Revealed by the USArray. *Earth Planet. Sci. Lett.* 402, 305–312. doi:10.1016/j.epsl.2013.02.015

Oganov, A. R., Ono, S., Ma, Y., Glass, C. W., and Garcia, A. (2008). Novel High-Pressure Structures of MgCO3, CaCO3 and CO2 and Their Role in Earth's Lower Mantle. *Earth Planet. Sci. Lett.* 273, 38–47. doi:10.1016/j.epsl.2008.06.005

Palyanov, Y. N., Sokol, A. G., Borzdov, Y. M., Khokhryakov, A. F., and Sobolev, N. V. (2002). Diamond Formation Through Carbonate-Silicate Interaction. *Am. Mineral.* 87, 1009–1013. doi:10.2138/am-2002-0726

Palyanov, Y. N., Bataleva, Y. V., Sokol, A. G., Borzdov, Y. M., Kupriyanov, I. N., Reutsky, V. N., et al. (2013). Mantle-slab Interaction and Redox Mechanism of Diamond Formation. *Proc. Natl. Acad. Sci.* 110 (51), 20408–20413. doi:10.1073/pnas.1313340110

Panero, W. R., and Kabbes, J. E. (2008). Mantle-wide Sequestration of Carbon in Silicates and the Structure of Magnesite II. *Geophys. Res. Lett.* 35, L14307. doi:10.1029/2008gl034442

Pickard, C. J., and Needs, R. J. (2015). Structures and Stability of Calcium and Magnesium Carbonates at Mantle Pressures. *Phys. Rev. B* 91, 104101. doi:10.1103/physrevb.91.104101

Plank, T., and Langmuir, C. H. (1993). Tracing Trace Elements from Sediment Input to Volcanic Output at Subduction Zones. *Nature* 362, 739–743. doi:10.1038/362739a0

Rohrbach, A., and Schmidt, M. W. (2011). Redox Freezing and Melting in the Earth's Deep Mantle Resulting from Carbon-Iron Redox Coupling. *Nature* 472, 209–212. doi:10.1038/nature09899

Santillán, J., Williams, Q., and Knittle, E. (2003). Dolomite-II: A High-Pressure Polymorph of $CaMg(CO_3)_2$. *Geophys. Res. Lett.* 30 (2), 1054. doi:10.1029/2001GL016018

Santos, S. S. M., Marcondes, M. L., Justo, J. F., and Assali, L. V. C. (2019). Stability of Calcium and Magnesium Carbonates at Earth's Lower Mantle Thermodynamic Conditions. *Earth Planet. Sci. Lett.* 506, 1–7. doi:10.1016/j.epsl.2018.10.030

Shatskiy, A., Bekhtenova, A., Podborodnikov, I. V., Arefiev, A. V., Vinogradova, Y. G., and Litasov, K. D. (2021). Solidus of Carbonated Phlogopite Eclogite at 3-6 GPa: Implications for Mantle Metasomatism and Ultra-high Pressure Metamorphism. *Gondwana Res.* 103, 188–204. doi:10.1016/j.gr.2021.10.016

Smith, D., Lawler, K. V., Martinez-Canales, M., Daykin, A. W., Fussell, Z., Alexander, S. G., et al. (2018). Postaragonite Phases of $CaCO_3$ at Lower Mantle Pressures. *Phys. Rev. Mater.* 2, 013605. doi:10.1103/physrevmaterials.2.013605

Smith, E. M., Shirey, S. B., Nestola, F., Bullock, E. S., Wang, J., Richardson, S. H., et al. (2016). Large Gem Diamonds from Metallic Liquid in Earth's Deep Mantle. *Science* 354 (6318), 1403–1405. doi:10.1126/science.aal1303

Solomatova, N. V., and Asimow, P. D. (2016). *Ab Initio Study of the Structure and Stability of High-Pressure Iron-Bearing Dolomite*. American Geophysical Union, Fall Meeting.

Solopova, N. A., Dubrovinsky, L., Spivak, A. V., Litvin, Y. A., and Dubrovinskaia, N. (2015). Melting and Decomposition of MgCO3 at Pressures up to 84 GPa. *Phys. Chem. Minerals* 42, 73–81. doi:10.1007/s00269-014-0701-1

Spivak, A., Solopova, N., Litvin, L., and Dubrovinsky, L. (2013). Chemical Interaction of Mg-Carbonate and the Earth's Lower Mantle Minerals. EGU General Assembly. *Geophys. Res. Abstr.* 15, EGU2013–44741.

Spivak, A., Solopova, N., Cerantola, V., Bykova, E., Zakharchenko, E., Dubrovinsky, L., et al. (2014). Raman Study of MgCO3-FeCO3 Carbonate Solid Solution at High Pressures up to 55 GPa. *Phys. Chem. Minerals* 41, 633–638. doi:10.1007/s00269-014-0676-y

Spivak, A. V., Dubrovinskii, L. S., and Litvin, Y. A. (2011). Congruent Melting of Calcium Carbonate in a Static experiment at 3500 K and 10-22 GPa: Its Role in the Genesis of Ultradeep Diamonds. *Dokl. Earth Sc.* 439 (2), 1171–1174. doi:10.1134/s1028334x11080319

Stachel, T., and Harris, J. W. (2008). The Origin of Cratonic Diamonds - Constraints from Mineral Inclusions. *Ore Geology. Rev.* 34, 5–32. doi:10.1016/j.oregeorev.2007.05.002

Stagno, V., Tange, Y., Miyajima, N., McCammon, C. A., Irifune, T., and Frost, D. J. (2011). The Stability of Magnesite in the Transition Zone and the Lower Mantle as Function of Oxygen Fugacity. *Geophys. Res. Lett.* 38, L19309. doi:10.1029/2011gl049560

Stekiel, M., Girard, A., Nguyen-Thanh, T., Bosak, A., Milman, V., and Winkler, B. (2019). Phonon-driven Phase Transitions in Calcite, Dolomite, and Magnesite. *Phys. Rev. B* 99, 054101. doi:10.1103/physrevb.99.054101

Stekiel, M., Nguyen-Thanh, T., Chariton, S., McCammon, C., Bosak, A., Morgenroth, W., et al. (2017). High Pressure Elasticity of FeCO 3 -MgCO 3 Carbonates. *Phys. Earth Planet. Interiors* 271, 57–63. doi:10.1016/j.pepi.2017.08.004

Sun, W.-d., Hawkesworth, C. J., Yao, C., Zhang, C.-c., Huang, R.-f., Liu, X., et al. (2018). Carbonated Mantle Domains at the Base of the Earth's Transition Zone. *Chem. Geology.* 478, 69–75. doi:10.1016/j.chemgeo.2017.08.001

Syracuse, E. M., van Keken, P. E., and Abers, G. A. (2010). The Global Range of Subduction Zone Thermal Models. *Phys. Earth Planet. Interiors* 183, 73–90. doi:10.1016/j.pepi.2010.02.004

Takafuji, N., Fujino, K., Nagai, T., Seto, Y., and Hamane, D. (2006). Decarbonation Reaction of Magnesite in Subducting Slabs at the Lower Mantle. *Phys. Chem. Minerals* 33, 651–654. doi:10.1007/s00269-006-0119-5

Tao, R., Zhang, L., Fei, Y., and Liu, Q. (2014). The Effect of Fe on the Stability of Dolomite at High Pressure: Experimental Study and Petrological Observation in Eclogite from Southwestern Tianshan, China. *Geochimica Et Cosmochimica Acta* 143, 253–267. doi:10.1016/j.gca.2014.02.031

Tao, R., Zhang, L., and Zhang, L. (2020). Redox Evolution of Western Tianshan Subduction Zone and its Effect on Deep Carbon Cycle. *Geosci. Front.* 11 (3), 915–924. doi:10.1016/j.gsf.2019.09.007

Thomson, A. R., Walter, M. J., Kohn, S. C., and Brooker, R. A. (2016). Slab Melting as a Barrier to Deep Carbon Subduction. *Nature* 529, 76–79. doi:10.1038/nature16174

Tomlinson, E. L., Howell, D., Jones, A. P., and Frost, D. J. (2011). Characteristics of HPHT Diamond Grown at Sub-lithosphere Conditions (10-20GPa). *Diamond Relat. Mater.* 20, 11–17. doi:10.1016/j.diamond.2010.10.002

Weis, C., Sternemann, C., Cerantola, V., Sahle, C. J., Spiekermann, G., Harder, M., et al. (2017). Pressure Driven Spin Transition in Siderite and Magnesiosiderite Single Crystals. *Sci. Rep.* 7, 16526. doi:10.1038/s41598-017-16733-3

Yang, J., Mao, Z., Lin, J.-F., and Prakapenka, V. B. (2014). Single-crystal Elasticity of the Deep-Mantle Magnesite at High Pressure and Temperature. *Earth Planet. Sci. Lett.* 392, 292–299. doi:10.1016/j.epsl.2014.01.027

Yang, Z., and He, X. (2015). Oceanic Crust in the Mid-mantle Beneath West-central Pacific Subduction Zones: Evidence fromStoPconverted Waveforms. *Geophys. J. Int.* 203 (1), 541–547. doi:10.1093/gji/ggv314

Zhang, Z. G., Mao, Z., Liu, X., Zhang, Y. G., and Brodholt, J. (2018b). Stability and Reactions of $CaCO_3$ Polymorphs in the Earth's Deep Mantle. *J. Geophys. Research-Solid Earth* 123, 6491–6500. doi:10.1002/2017jb015019

Zhang, Z., Hastings, P., Von der Handt, A., and Hirschmann, M. M. (2018a). Experimental Determination of Carbon Solubility in Fe-Ni-S Melts. *Geochimica Et Cosmochimica Acta* 225, 66–79. doi:10.1016/j.gca.2018.01.009

Zhang, Z., and Liu, Z. (2015). High Pressure Equation of State for Molten CaCO3 from First Principles Simulations. *Chin. J. Geochem.* 34 (1), 13–20. doi:10.1007/s11631-015-0036-8

Zhao, S., Schettino, E., Merlini, M., and Poli, S. (2019). The Stability and Melting of Aragonite: An Experimental and Thermodynamic Model for Carbonated Eclogites in the Mantle. *Lithos* 324-325, 105–114. doi:10.1016/j.lithos.2018.11.005

Zhu, F., Li, J., Liu, J. C., Lai, X. J., Chen, B., and Meng, Y. (2018). Kinetic Control on the Depth Distribution of Superdeep Diamonds. *Geophys. Res. Lett.* 46, 1984–1992. doi:10.1029/2018GL080740

Zhu, Y.-F., Massonne, H.-J., and Men-Fan Zhu, M. F. (2009). Petrology of Low-Temperature, Ultrahigh-Pressure Marbles and Interlayered Coesite Eclogites Near Sanqingge, Sulu Terrane, Eastern China. *Mineral. Mag.* 73 (2), 307–332. doi:10.1180/minmag.2009.073.2.307

Conflict of Interest: The authors declare that the research was conducted in the absence of any commercial or financial relationships that could be construed as a potential conflict of interest.

Publisher's Note: All claims expressed in this article are solely those of the authors and do not necessarily represent those of their affiliated organizations, or those of the publisher, the editors and the reviewers. Any product that may be evaluated in this article, or claim that may be made by its manufacturer, is not guaranteed or endorsed by the publisher.